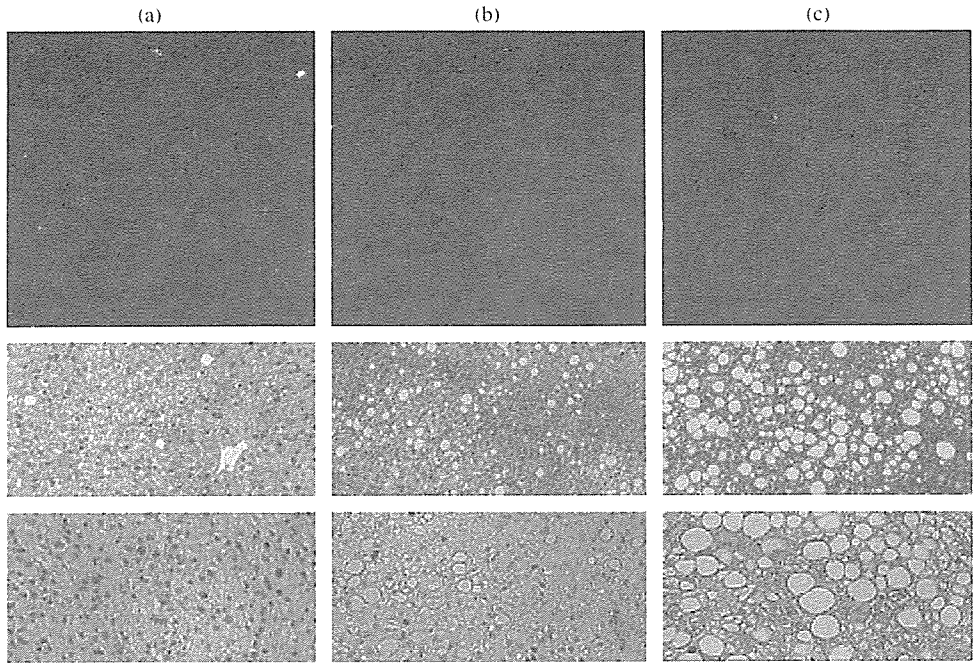

Fig. 2. Representative photographs of quantitative fluorescence *in situ* hybridization (upper), hematoxylin and eosin (HE) staining (middle) and Ki-67 immunostaining (bottom). The Tel(H)/Tel(L) calculated for one field of view from samples (a) control group, (b) group A and (c) group B were 1.633 (Tel(H) = 0.119 ± 0.027, Tel(L) = 0.073 ± 0.044), 1.850 (Tel(H) = 0.107 ± 0.029, Tel(L) = 0.058 ± 0.024) and 0.678 (Tel(H) = 0.043 ± 0.006, Tel(L) = 0.063 ± 0.024), respectively.

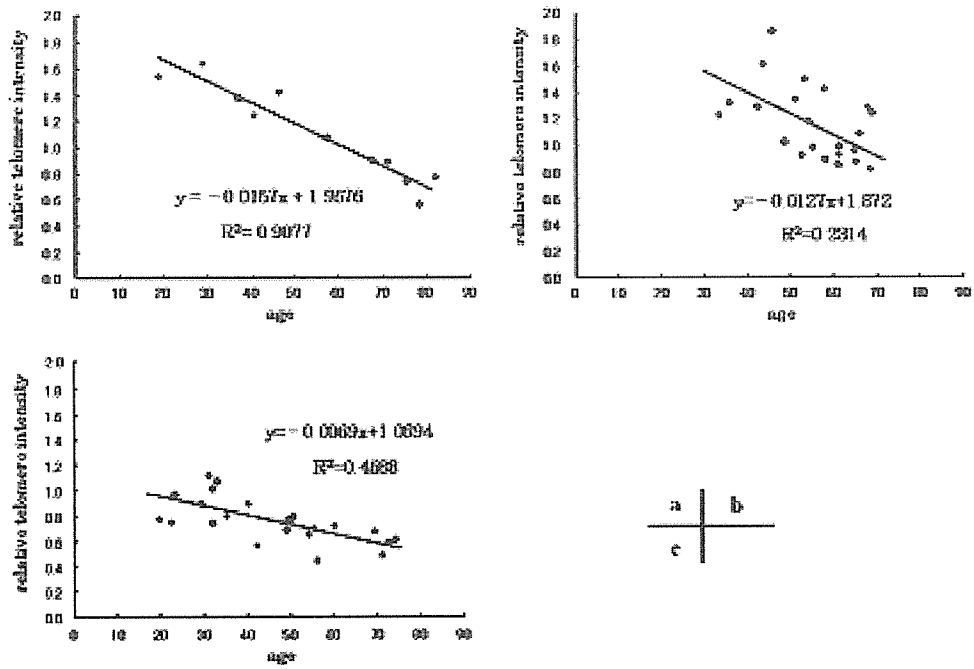

Fig. 3. Telomeric pixel intensities of individual hepatocyte and lymphocyte nuclei were recorded in samples from normal individuals, group A and group B patients. For each field, the value derived from the adjusted telomeric signal intensities of each hepatocyte nucleus or each lymphocyte nucleus was designated Tel-H or Tel-L, respectively. The ratio of mean Tel-H/mean Tel-L was calculated for each field after assessing 15–20 hepatocytes and more than 10 lymphocytes. Relative telomere intensity was determined by the average value of mean Tel-H/mean Tel-L following analysis of at least 5 different fields per sample. (a) The slope of the linear regression for age vs relative telomere intensity in normal individuals was calculated to be $y = -0.0157x+1.9576$, where x was patient's age and y was the relative telomere intensity. Those with liver biopsies at least 80% of the normal ratio of relative telomere intensity to age were classified into group A, and those showing less than 80% of the normal ratio were designated group B. (b) Group A. Several group A patients of all ages showed normal telomere length. The slope of the linear regression for age vs relative telomere intensity was calculated to be $y = -0.0127x+1.872$. (c) Group B. The telomere lengths of some patients in group B were already shortened remarkably in early age. The slope of the linear regression for age vs relative telomere intensity was calculated to be $y = -0.0069x+1.0694$.

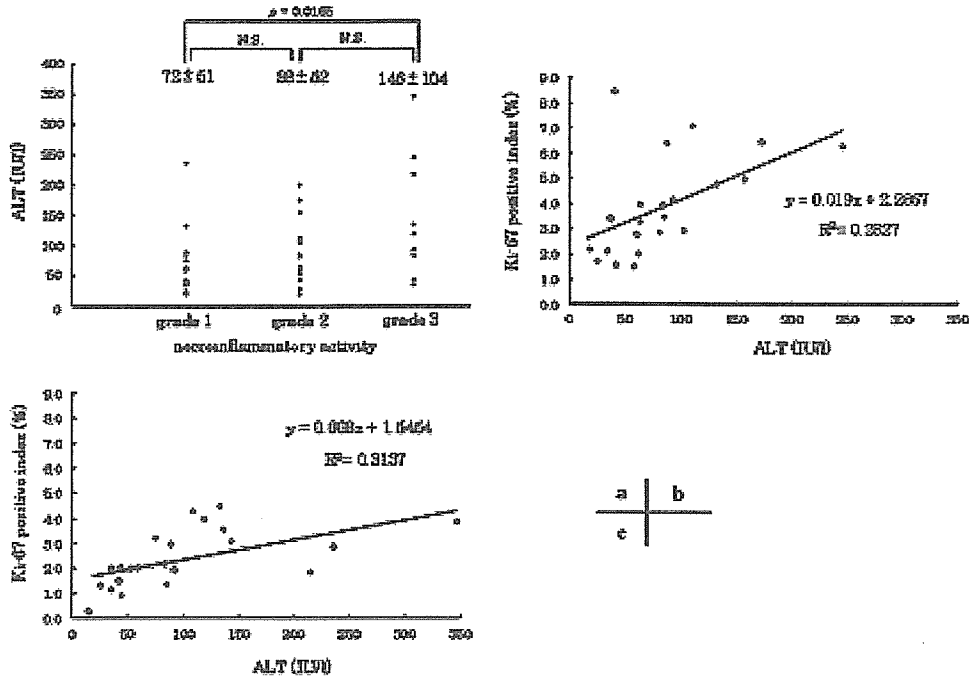

Fig. 4. (a) The mean alanine aminotransferase (ALT) values were higher in samples scored as Brunt's necroinflammatory grade 3 compared with those of grade 1 ($P = 0.0165$ by t test). A trend could be seen in ALT with higher values in the higher grades among all NAFLD patients tested (by $P = 0.0846$ Kruskal–Wallis analysis). NS, not significant. (b) The Ki-67-PI and ALT value were closely correlated in group A, and also (c) in group B, indicating that regenerative proliferation is reactive to necroinflammation in both groups. The group B values for both the Ki-67 positive index and the ratio of Ki-67-PI to ALT were significantly lower than group A ($P = 0.0046$ and 0.0003, respectively by Mann–Whitney analysis), suggesting that the hepatocellular replicative response of group B is depressed relative to group A.

Table 1. Clinicopathological summary of groups A and B. Data were presented as means ± standard deviations

	Group A	Group B	*P*-value
HOMA-IR	2.2 ± 1.3	3.7 ± 1.9	0.0190
BMI	25.7 ± 2.9	28.9 ± 5.6	0.0232
Hepatic steatosis (%)	43 ± 19	57 ± 23	0.0364
Grade of inflammation	1.54 ± 0.60	1.77 ± 0.61	0.2093
Stage of fibrosis	1.22 ± 1.27	1.27 ± 1.12	0.7414
ALT (IU/l)	84 ± 54	100 ± 80	0.7159
Ki-67-PI (%)	3.9 ± 1.9	2.4 ± 1.1	0.0046
Ki-67-PI (%)/ALT (IU/l)	0.057 ± 0.039	0.043 ± 0.032	0.0003
8-HdG immunostaining grade	1.95 ± 0.80	2.62 ± 0.67	0.0059

Mann–Whitney test was used for statistical analysis of difference between two groups. HOMA-IR homeostasis model assessment insulin resistance; BMI, body mass index; ALT, alanine aminotransferase; Ki-67-PI, Ki-67-positive index; 8-OHdG, 8-hydroxy-2′-deoxyguanosine.

group, group A and group B were 0.85, 0.98 and 0.59, respectively.

Overall, values for HOMA-IR and BMI were significantly higher in group B than in group A ($P = 0.0190$ and 0.0232, respectively, by Mann–Whitney analysis, Table 1). The percent fat in each section was 43.2 ± 18.6% in group A and 57.0 ± 22.6% in group B. Therefore, hepatic steatosis was also significantly more severe in group B than group A ($P = 0.0364$ by Mann–Whitney analysis, Table 1). Immunoreactivity of 8-OHdG in hepatocytes was graded as 1.95 ± 0.80 in group A and 2.62 ± 0.67 in group B. Hence, 8-OHdG expression was significantly more intense in group B than group A ($P = 0.0059$ by Mann–Whitney analysis, Table 1). Of seven group B patients less than 40 years old, the 8-OHdG levels of five were grade 3 and of two were grade 2. On the other hand, of two similarly aged patients in group A, one was grade 1 and another was grade 2. There were no significant differences in the degree of inflammation, the stage of fibrosis, or the ALT values (Table 1). The mean ALT values were higher in patients displaying Brunt's necroinflammatory rating of grade 3 compared with grade 1 ($P = 0.0165$ by t test). There was a positive correlation between high ALT values and high necroinflammatory grades among all NAFLD patients tested ($P = 0.0846$ by Kruskal–Wallis analysis, Fig. 4a). Furthermore, there was a positive correlation between Ki-67-PI and ALT values within group A (Fig. 4b, $R^2 = 0.2827$, $P < 0.05$, $n = 22$) and group B (Fig. 4c, $R^2 = 0.3137$, $P < 0.01$, $n = 22$), however group B values for both the Ki-67 positive index and the ratio of Ki-67-PI to ALT were significantly lower than group A ($P = 0.0046$ and 0.0003, respectively by Mann–Whitney analysis, Table 1). These data indicate that regenerative proliferation is generally stimulated in response to necroinflammation, but that the

hepatocellular replicative response of group B is depressed relative to group A.

Discussion

This report is the first to investigate the association between telomere shortening, hepatic steatosis and obesity in NAFLD. Our data show that group B NAFLD patients, in whom hepatocyte telomeres were significantly shorter than the group A or control patients of similar age, also were more resistant to insulin, more obese and showed a higher degree of hepatic steatosis than group A. Insulin resistance contributes to the increased entry of fat into hepatocytes by increasing the synthesis of free fatty acids (FFAs) from glucose not taken up by peripheral adipocytes and myocytes (24). Hepatic FFAs either undergo β-oxidation as part of the mitochondrial antioxidant defense system, or are converted to triglycerides. Some of these triglycerides accumulate as fat droplets in the cytoplasm, resulting in steatosis.

There are two probable causes for the telomere shortening demonstrated most prominently in young group B patients: abnormally high cell turnover and intracellular oxidative damage. Previous reports have shown that in virus-associated chronic hepatitis and liver cirrhosis (8–10), one effect of chronic hepatocellular necrosis is a high level of cellular regeneration. Although high levels of cell turnover may contribute to the premature telomere shortening seen in NAFLD, our data suggest that this effect is not likely to be the major cause of telomere shortening in young NAFLD patients, since hepatic fibrosis, which is generally considered as the result of long-term repeated cell-cycle turnover, was not significantly different between study groups.

Recently, it has been suggested that telomeres are shortened not only during cell division, but also by insufficient repair of ROS-mediated DNA damage in telomeres relative to elsewhere in the chromosome (11–13). Since it has been shown that mitochondrial function is impaired in patients with severe hepatic steatosis, with or without steatohepatitis (25, 26), we predict that hepatocellular FFA uptake in NAFLD patients is relatively high, resulting in increases in intracellular ROS. With this in mind, we hypothesize that oxidative damage caused by these high levels of intracellular ROS in NAFLD hepatocytes is a primary cause of shortened telomeres. Our data support this hypothesis, in that young group B patients, who showed a greater degree of hepatic steatosis and 8-OHdG expression than group A patients, also demonstrated the most prominent telomere shortening. In many kinds of chronic liver injury, the stage of fibrosis as a result of repeated cell-cycle turnover mainly causes telomere shortening of hepatocytes (10). In contrast, in NAFLD, the degree of steatosis, and not of fibrosis, seems to play a major role of telomere shortening. Therefore, NAFLD can be one of the rare human models of ROS-based telomere shortening of hepatocytes.

We assumed that telomeres are relatively stable in lymphocytes as this has been reported on healthy aging humans (23). Meanwhile, there is a report that the telomere length from white blood cells of patients with insulin-dependent diabetes mellitus (IDDM) was significantly shorter than that of nondiabetic control subjects but that no significant difference was observed between the telomere lengths from white blood cells of patients with noninsulin-dependent diabetes mellitus (NIDDM) vs nondiabetic subjects (27). In our study, there was no IDDM patient. However, it is still possible that disease conditions leading to NAFLD would not only affect the telomere lengths of hepatocytes but also those of lymphocytes, especially the lymphocytes infiltrating in the liver. Therefore, the degree of hepatocyte telomere shortening might be underestimated by measuring the relative telomere length of hepatocytes in relation to infiltrating lymphocytes.

Studies of NAFLD using animal model systems suggest an impaired capacity for hepatocellular regeneration. In experimental obese diabetic Zucker fa/fa rats with fatty livers, liver regeneration after two-thirds partial hepatectomy is inhibited (28). In mice with NAFLD, the hepatocellular response to acute regenerative stimuli is disrupted, and hepatocytes adopt adaptive signaling pathways to survive chronic oxidative stress (29). This study is the first to demonstrate that hepatocellular replication in human NAFLD subjects with shortened telomeres is less responsive to necroinflammation. We compared the replicative response in groups A and B in relation to telomere-associated cellular senescence. From the assays of NAFLD patient biopsies, we used the Ki-67-PI as an indicator of hepatocyte proliferative activity, and ALT as a measure of necroinflammatory activity. By calculating the relative ratio of Ki-67-PI to ALT values from a given sample, we could quantify the replicative response to liver cell injury. In both groups, there was a positive correlation between Ki-67-PI and ALT values, suggesting that the regenerative proliferation is reactive to necroinflammation in both groups. Although no significant difference was detected between the mean ALT values of groups A and B, the mean Ki-67-PI in group B was significantly lower than in group A. Consequently, the Ki-67-PI/ALT

value was also lower in group B. These results suggest that hepatocytes of group B with age-matched short telomere have lower regenerative response that may be associated with the feature of replicative senescence. Besides, this lower replicative response can result in slower age-dependent shortening of telomere at least in some group B patients, compared with group A patients. The poor regenerative response demonstrated by group B hepatocytes with severely shortened telomeres may be an indication that these cells are in a state of replicative senescence.

Hepatocytes display some morphological features of cellular senescence. Watanabe et al. (30) report that the mean nuclear area of hepatocytes remains relatively constant in subjects under 60 years of age, but increases in those over 60, probably due to polyploidization. In comparisons among subjects under 50 years of age, we observed that the mean nuclear area of group B was significantly (11.8%) larger than that of group A (data not shown). This result provides further evidence that hepatocytes with prematurely shortened telomeres show morphological signs of cellular senescence at an earlier age.

Cells with extremely short telomeres display characteristics of replicative senescence. The 80% cut-off value divides these cases accurately into two groups, one which shows short telomeres with poor replicative response and the other which shows normal or near-normal length telomeres with good replicative response. Relative to cut-off values of 65% and 85%, the 80% cut-off value divided subjects in groups A or B in a more statistically relevant way, in that the *P*-value of difference in Ki-67-PI or Ki-67-PI/ALT between groups A and B was lowest at 80%, and the R^2-value for the relationship between Ki-67-PI and ALT was highest within each group. Thus, we infer that the 80% cut-off value is biologically important and that the 44 cases were divided into two relevant groups: group A showing high replicative response and group B showing low response, with subjects in the same group displaying a similar degree of replicative response.

It has been suggested that the stage of NAFLD might advance when an acute or chronic inflammatory insult, i.e., 'second hit,' is superimposed on hepatic steatosis (31). A diseased liver consisting of senescent hepatocytes with insufficient regenerative capacity is vulnerable to the effect of a second-hit insult. With this in mind, the telomere shortening documented in group B patients should likely be viewed as a decisive 'first-hit.' Interestingly, however, our study showed no significant difference in the stage of fibrosis between groups A and B. One explanation for this may be that differences in the degree of necroinflammation following exposure to second-hit insults would affect the overt progression of NAFLD. Since our present data is based on a short-term study, it is not possible to predict whether group B patients would show a more rapid progression of fibrosis or whether telomere shortening affects overall clinical course. Adams et al. (32) has reported that diabetes, higher BMI and low initial fibrosis stage are all associated with an increased rate of fibrosis progression. Further follow-up and longitudinal studies of individual patients in our study will be needed to accurately determine the rate of progression of NAFLD patients with prominent telomere shortening.

References

1. Matteoni C A, Younossi Z M, Gramlich T, Boparai N, Liu Y C, McCullough A J. Non-alcoholic fatty liver disease: a spectrum of clinical and pathological severity. Gastroenterology 1999; 116: 1413–9.
2. Fassio E, Alvarez E, Dominquez N, Landeira G, Longo C. Natural history of nonalcoholic steatohepatitis: a longitudinal study of repeat liver biopsy. Hepatology 2004; 40: 820–6.
3. Hui J M, Kench J G, Chitturi S, Sud A, Farrell G C, Byth K, et al. Long-term outcomes of cirrhosis in nonalcoholic steatohepatitis compared with hepatitis C. Hepatology 2003; 38: 420–7.
4. Blackburn E H. Structure and function of telomeres. Nature 1991; 350: 569–73.
5. Levy M Z, Allsopp R C, Futcher A B, Greider C W, Harley C B. Telomere end-replication problem and cell aging. J Mol Biol 1992; 225: 951–60.
6. Blackburn E H. Switching and signaling at the telomere. Cell 2001; 106: 661–73.
7. Satyanarayana A, Wiemann S U, Buer J, Lauber J, Dittmar K E, Wustefeld T, et al. Telomere shortening impairs organ regeneration by inhibiting cell cycle re-entry of a subpopulation of cells. EMBO J 2003; 22: 4003–13.
8. Aikata H, Takaishi Y, Kawakami S, Takahashi M, Kitamoto T, Nakanishi Y, et al. Telomere reduction in human liver tissues with age and chronic inflammation. Exp Cell Res 2000; 256: 578–82.
9. Paradis V, Youssef N, Dargere D, Ba N, Bonvoust F, Deschatrette J, et al. Replicative senescence in normal liver, chronic hepatitis C, and hepatocellular carcinomas. Hum Pathol 2001; 32: 327–32.
10. Wiemann S U, Satyanarayana A, Tsahuridu M, Tillmann H L, Zender L, Klempnauer J, et al. Hepatocyte telomere shortening and senescence are general markers of human liver cirrhosis. FASEB J 2002; 16: 935–42.
11. von Zglinicki T. Oxidative stress shortens telomeres. Trends Biochem Sci 2002; 27: 339–44.
12. Saretzki G, Von Zglinicki T. Replicative aging, telomeres, and oxidative stress. Ann NY Acad Sci 2002; 959: 24–9.
13. Kawanishi S, Oikawa S. Mechanism of telomere shortening by oxidative stress. Ann NY Acad Sci 2004; 1019: 278–84.
14. Meeker A K, Gage W R, Hicks J L, Simon I, Coffman J R, Platz E A, et al. Telomere length assessment in human archival tissues: combined telomere fluorescence in situ

hybridization and immunostaining. Am J Pathol 2002; 160: 1259–68.
15. Ferlicot S, Youssef N, Feneux D, Delhommeau F, Paradis V, Bedossa P. Measurement of telomere length on tissue sections using quantitative fluorescence in situ hybridization (Q-FISH). J Pathol 2003; 200: 661–6.
16. Kapoor V, Telford W G. Telomere length measurement by fluorescence in situ hybridization and flow cytometry. Methods Mol Biol 2004; 263: 385–98.
17. Neuschwander-Tetri B A, Caldwell S H. Nonalcoholic steatohepatitis: summary of an AASLD single topic conference. Hepatology 2003; 37: 1202–19.
18. Brunt E M, Janney C G, Di Bisceglie A M, Neuschwander-Tetri B A, Bacon B R. Nonalcoholic steatohepatitis: a proposal for grading and staging the histological lesions. Am J Gastroenterol 1999; 94: 2467–74.
19. Matthews D R, Hosker J P, Rudenski A S, Naylor B A, Treacher D F, Turner R C. Homeostasis model assessment: insulin resistance and beta-cell function from fasting plasma glucose and insulin concentrations in man. Diabetologia 1985; 28: 412–9.
20. Mizuno T, Matsui H, Imamura A, Numaguchi Y, Sakai K, Murohara T, et al. Insulin resistance increases circulating malondialdehyde-modified LDL and impairs endothelial function in healthy young men. Int J Cardiol 2004; 97: 455–61.
21. Shiomoda R, Nagashima M, Sakamoto M, Yamaguchi N, Hirohashi S, Yokota J, et al. Increased formation of oxidative DNA damage, 8-hydroxydeoxyguanosine, in human livers with chronic hepatitis. Cancer Res 1994; 54: 3171–2.
22. Kato J, Kobune M, Nakamura T, Kuroiwa G, Takada K, Takimoto R, et al. Normalization of elevated hepatic 8-hydroxy-2′-deoxyguanosine levels in chronic hepatitis C patients by phlebotomy and low iron diet. Cancer Res 2001; 61: 8697–702.
23. Iwama H, Ohyashiki K, Ohyashiki J H, Hayashi S, Yahata N, Ando K, et al. Telomeric length and telomerase activity vary with age in peripheral blood cells obtained from normal individuals. Hum Genet 1998; 102: 397–402.
24. Fromenty B, Robin M A, Igoudjil A, Mansouri A, Pessayre D. The ins and outs of mitochondrial dysfunction in NASH. Diabetes Metab 2004; 30: 121–38.
25. Baffy G, Zhang C Y, Glickman J N, Lowell B B. Obesity-related fatty liver is unchanged in mice deficient for mitochondrial uncoupling protein 2. Hepatology 2002; 35: 753–61.
26. Spahr L, Negro F, Leandro G, Marinescu O, Goodman K J, Rubbia-Brandt L, et al. Impaired hepatic mitochondrial oxidation using the 13C-methionine breath test in patients with macrovesicular steatosis and patients with cirrhosis. Med Sci Monit 2003; 9: 6.
27. Jeanclos E, Krolewski A, Skurnick J, Kimura M, Aviv H, Warram J H, et al. Shortened telomere length in white blood cells of patients with IDDM. Diabetes 1998; 47: 482–6.
28. Diehl A M. Animal models of hepatic steatosis. Semin Liver Dis 2001; 21: 89–104.
29. Yang S Q, Lin H Z, Mandal A K, Huang J, Diehl A M. Disrupted signaling and inhibited regeneration in obese mice with fatty livers: implications for nonalcoholic fatty liver disease pathophysiology. Hepatology 2001; 34: 694–706.
30. Watanabe T, Shimada H, Tanaka Y. Human hepatocytes and aging: a cytophotometrical analysis in 35 sudden-death cases. Virchows Arch B Cell Pathol 1978; 27: 307–16.
31. Day C P, James O F. Steatohepatitis: a tale of two 'hits'? Gastroenterology 1998; 114: 842–5.
32. Adams L A, Sanderson S, Lindor K D, Angulo P. The histological course of nonalcoholic fatty liver disease: a longitudinal study of 103 patients with sequential liver biopsies. J Hepatol 2005; 42: 132–8.

Liver International 2006: 26: 613–620

Liver International
DOI: 10.1111/j.1478-3231.2006.01265.x

Basic Studies

Fenofibrate, a peroxisome proliferator-activated receptor α agonist, reduces hepatic steatosis and lipid peroxidation in fatty liver Shionogi mice with hereditary fatty liver

Harano Y, Yasui K, Toyama T, Nakajima T, Mitsuyoshi H, Mimani M, Hirasawa T, Itoh Y, Okanoue T. Fenofibrate, a peroxisome proliferator-activated receptor α agonist, reduces hepatic steatosis and lipid peroxidation in fatty liver shionogi mice with hereditary fatty liver.
Liver International 2006: 26: 613–620.

Abstract: *Background and aims:* The fatty liver Shionogi (FLS) mouse, a unique model for nonalcoholic fatty liver disease (NAFLD), is an inbred strain that develops spontaneous hepatic steatosis without obesity or diabetes mellitus. Peroxisome proliferator-activated receptor (PPAR) α controls fatty acid metabolism. In the present study, we investigated the effect of fenofibrate, a PPARα agonist, on hepatic steatosis in FLS mice. *Methods:* Thirteen-week-old FLS mice were fed a diet with 0.1% fenofibrate (w/w) for 12 days. The degree of hepatic steatosis was estimated by histological examination and hepatic triglyceride levels. Expression levels of genes involved in fatty acid turnover, including *Acox1*, *Cpt1a*, *Fabp1*, *Acadl*, and *Acadm*, were determined by Northern blot analyses. We measured levels of lipid peroxidation, glutathione, and anti-oxidative enzymes, such as superoxide dismutase, catalase, and glutathione peroxidase, in the liver. *Result:* Treatment of FLS mice with fenofibrate improved hepatic steatosis by activating expression of genes involved in fatty acid turnover and decreased hepatic lipid peroxidation. Fenofibrate increased the activity of catalase by upregulating its mRNA levels. *Conclusion:* Fenofibrate, which is currently used in therapy of hyperlipidemia, might also be useful for treating patients with NAFLD even in cases where NAFLD is not associated with obesity or diabetes mellitus.

Yuichi Harano[1], Kohichiroh Yasui[1], Tetsuya Toyama[1], Tomoki Nakajima[1], Hironori Mitsuyoshi[1], Masahito Mimani[1], Tsutomu Hirasawa[2], Yoshito Itoh[1] and Takeshi Okanoue[1]

[1]Molecular Gastroenterology and Hepatology, Graduate School of Medical Science, Kyoto Prefectural University of Medicine, Kyoto, Japan, [2]Aburahi Laboratories, Shionogi & Co. Ltd., Shiga, Japan

Key words: catalase – fenofibrate – FLS mouse – hepatic steatosis – lipid peroxidation – oxidative stress – PPARα

Takeshi Okanoue, MD, Molecular Gastroenterology and Hepatology, Graduate School of Medical Science, Kyoto Prefectural University of Medicine, Kawaramachi-Hirokoji, Kamigyo-ku, Kyoto 602-8566, Japan.
Tel: +81 75 251 5519
Fax: +81 75 251 0710
e-mail: okanoue@koto.kpu-m.ac.jp

Received 17 November 2005,
accepted 26 February 2006

Nonalcoholic fatty liver disease (NAFLD) is one of the most common causes of chronic liver disease and is frequently associated with obesity, insulin resistance, and type 2 diabetes mellitus (1–7). The spectrum of NAFLD ranges from simple steatosis to nonalcoholic steatohepatitis (NASH), which can progress to liver cirrhosis and hepatocellular carcinoma. Although the etiopathogenesis of NASH remains poorly understood, a two-hit theory has been proposed (8–10). The first hit is represented by excessive fat accumulation in the liver, and the second hit is mainly related to increased intrahepatic oxidative stress and endotoxin-induced cytokines (9–11).

The fatty liver shionogi (FLS) mouse is an inbred strain that develops spontaneous hepatic steatosis (12). Although FLS mice show no hyperphagia, obesity, or diabetes mellitus, they do show accumulation of lipid droplets in the hepatocytes, beginning at least from the time of birth, and develop severe chronic fatty liver under normal conditions. Hepatic steatosis in FLS mice is considered to be a complex polygenetic trait (12). Moreover, FLS mice older than 1 year frequently develop hepatocellular adenoma and/or carcinoma subsequent to steatohepatitis (13). Therefore, the FLS mouse appears to be a good animal model for studying NAFLD, especially NAFLD unrelated to

obesity or diabetes mellitus. Indeed, a significant portion of patients with NAFLD do not have obesity or diabetes mellitus (5, 6).

The peroxisome proliferator-activated receptors (PPARs) belong to the superfamily of ligand-activated nuclear hormone receptors that regulate energy homeostasis (14–17). Three PPAR isotypes, PPARα, PPARβ, and PPARγ, are found in most vertebrates, including humans and other mammals (18, 19). PPARα is predominantly expressed in the liver, kidney, heart, and skeletal muscle, where it controls fatty acid catabolism (17, 20–25). The metabolism of fatty acid in the liver is regulated by PPARα. Fibrates, such as fenofibrate and bezafibarate, are well-known PPARα agonists and are used for treating dyslipidemia (26). Some investigators have shown that PPARα agonists prevent and/or improve hepatic steatosis in animal models of NAFLD (27, 28). Our earlier study revealed that two PPARα agonists, Wy-14643 and fenofibrate, suppress hepatic fibrosis in a thioacetamide model of liver cirrhosis in rats by activating antioxidative enzymes (29).

In the present study, we investigated the effect of fenofibrate on hepatic steatosis in the FLS mouse. Our data showed that fenofibrate improved hepatic steatosis by activating expression of genes involved in fatty acid turnover. Furthermore, fenofibrate reduced hepatic lipid peroxidation by activating catalase, an antioxidative enzyme, in addition to improving steatosis.

Materials and methods

Animals and experimental protocols

Male FLS and dd Shionogi (DS) mice used in this study were previously established and described (12). The DS mouse, a sister strain of the FLS mouse, did not manifest liver abnormality and thus was used as a control. Mice were caged individually, maintained on a 12-h light/dark cycle (6:00–18:00 hours), and fed standard chow diet (CA-1; Clea Japan Inc., Tokyo, Japan) containing 4.8% crude fat *ad libitum*. Thirteen-week-old FLS and DS mice were fed a CA-1 diet with or without 0.1% fenofibrate (Kaken Seiyaku Ltd., Tokyo, Japan) (w/w) for 12 days. All procedures were performed according to the experimental protocols approved by the Ethical Committee for Animal Experiments of Kyoto Prefectural University of Medicine.

Preparation of tissue and serum samples

Mice were anesthetized in the nonfasted state between 9:00 and 12:00 on day 12 of fenofibrate treatment. Blood was collected by cardiac puncture, and livers were rapidly excised and weighed. A portion of liver was processed for histopathologic studies, and the remainder was snap-frozen in liquid nitrogen and stored at −80 °C until assayed.

Histopathologic examinations

Liver tissues were fixed overnight at 4 °C in 4% paraformaldehyde dissolved in phosphate-buffered saline. The tissue was dehydrated, paraffin-embedded, and cut into sections. Liver sections were then stained with hematoxylin and eosin (HE) and oil red O (detection of lipids).

Biochemical assays

Serum triglyceride, total cholesterol, free fatty acid, aspartate aminotransferase (AST), and alanine aminotransferase (ALT) levels were measured by routine laboratory methods. Liver triglycerides were extracted from liver homogenates using methanol-chloroform (30) and quantitated using L-type Wako TG-H reagents (Wako Pure Chemical Industries Ltd., Osaka, Japan). Liver lipid peroxidation was estimated from the levels of malondialdehyde (MDA), which were measured by the thiobarbituric acid reduction method using an LPO-583 colorimetric kit (Oxis International, Portland, OR). Glutathione (GSH) levels in the liver were determined using a Bioxytech GSH-420 colorimetric kit (Oxis International). Cu/Zn-superoxide dismutase (SOD) and glutathione peroxidase (GPx) activities in liver homogenates were measured with spectrophotometric assay kits (Bioxytech SOD-525 and GPx-340, respectively; Oxis International) according to the manufacturer's instructions. Catalase activity was measured using the spectrophotometric method of Beers and Sizer (31) and expressed as U/mg protein as described by Aebi (32).

Northern blot analyses

Total RNA from the liver was isolated using the TRIzol reagent (Invitrogen, Tokyo, Japan). Twenty micrograms of total RNA derived from each one mouse was separated on a 1.2% agarose gel containing 2.2 M formaldehyde and then transferred onto a Hybond N+ nylon membrane (Amersham Biosciences Corp., Piscataway, NJ) by capillary blotting. We designed specific primers for the following genes and used the PCR products as probes: (1) acyl-coenzyme A oxidase 1, palmitoyl (*Acox1*, gene symbol; AOX, enzyme); (2) carnitine palmitoyltransferase 1a, liver (*Cpt1a*; CPT-1); (3) fatty acid binding protein 1,

liver (*Fabp1*; L-FABP); (4) acyl-coenzyme A dehydrogenase, long chain (*Acadl*; LCAD); (5) acyl-coenzyme A dehydrogenase, medium chain (*Acadm*; MCAD); (6) catalase (*Cat*); and (7) superoxide dismutase 1, soluble (*Sod1*; Cu/Zn-SOD). Primer sequences are available on request. The probe for PPARα (*Ppara*) was a gift from Dr. Wan (33). Probes were labeled with [α-^{32}P]dCTP by random priming (Megaprime; Amersham, Piscataway, NJ). Northern hybridization was performed in Ultrahyb solution (Ambion, Austin, TX) according to the manufacturer's instructions. Glyceraldehyde-3-phosphate dehydrogenase (*Gapdh*) was used as a control probe to estimate loading differences on the blots. Membranes were subjected to autoradiography at −80 °C overnight, using Kodak Biomax film (Tokyo, Japan), and hybridization signals were measured with a densitometric image analyzer (Atto, Tokyo, Japan). Expression levels were quantified by normalizing of gene-specific signals to *Gapdh* signal.

Statistical analysis

Results are expressed as the mean ± SD. Statistical differences between means were determined using Student's *t*-test and a one-way ANOVA (with appropriate *post hoc* analysis) for multiple comparisons. *P*-values $<.05$ were considered statistically significant.

Results

Effects of fenofibrate on hepatic steatosis in FLS mice

As reported previously (12), histological examination revealed that the liver from 15-week-old untreated FLS mice showed large lipid droplets throughout the lobes (Fig. 1B), whereas few fatty vesicles were observed in the liver of control DS mice (Fig. 1A). Fenofibrate led to disappearance of vacuolization in the liver of FLS mice (Fig. 1D). An oil red O staining confirmed that the vacuoles visible in the HE staining were lipid droplets (Fig. 1E–H). In both DS and FLS mice, fenofibrate treatment increased absolute and relative liver weights (Table 1), a known effect of the hepatocyte hypertrophy and hyperplasia caused by PPARα agonists in mice (Fig. 1C, D) (27, 34, 35).

Fenofibrate decreases hepatic triglyceride content in FLS mice

Hepatic triglyceride content was roughly fourfold higher in 13-week-old FLS mice than in age-matched DS mice (Fig. 2). A further increase in hepatic triglyceride content was observed in FLS mice aged 15 weeks. Its content was roughly eightfold higher in 15-week-old FLS mice than in DS mice (Fig. 2). In 15-week-old FLS mice, hepatic triglyceride levels were remarkably reduced by fenofibrate treatment (Fig. 2). This result is compatible with histological findings that fatty vesicles disappeared in the liver of fenofibrate-treated FLS mice (Fig. 1B, D, F, H). As summarized in Table 1, fenofibrate lowered serum levels of triglyceride and free fatty acid in both DS and FLS mice, and reduced serum total cholesterol levels in DS but not in FLS mice. Serum ALT levels were higher in FLS than DS mice. Treatment with fenofibrate induced no significant changes in the levels of AST or ALT in FLS mice; however, it elevated ALT levels in DS mice.

Fenofibrate induces the transcription of genes involved in fatty acid turnover

The reduced hepatic triglyceride levels could be accounted for by increased fatty acid oxidation, a known effect of PPARα agonists achieved via increased transcription of peroxisomal and mitochondrial β-oxidation genes (27, 28, 36). Therefore, we examined expression levels of the following genes that were involved in fatty acid turnover in the liver (*Acox1*, *Cpt1a*, *Fabp1*, *Acadl*, and *Acadm*) and PPARα (*Ppara*). Northern blot analyses showed no significant differences in expression levels for these six genes between untreated DS and FLS mice (Fig. 3). In FLS as well as DS mice, fenofibrate treatment induced the transcription of all six genes studied: *Acox1* (about 12-fold), *Cpt1a* (eightfold), *Fabp1* (sixfold), *Acadl* (fivefold), *Acadm* (eightfold), and *Ppara* (threefold) (Fig. 3).

Effect of fenofibrate on lipid peroxidation in the liver

Because several lines of evidence have shown that hepatic steatosis leads to lipid peroxidation in mice (28, 37), we determined the degree of hepatic lipid peroxidation in FLS mice. Levels of MDA, a marker for lipid peroxidation, were 1.7-fold higher in the liver of FLS mice than in DS mice, indicating that hepatic lipid peroxidation occurred in FLS mice (Fig. 4A). We next examined whether fenofibrate had effects on hepatic lipid peroxidation. Fenofibrate significantly reduced MDA levels in the FLS mice (Fig. 4A).

To investigate the mechanism by which fenofibrate decreased lipid peroxidation in FLS mice, we determined the activities of antioxidative enzymes, including catalase, Cu/Zn-SOD, and glutathione peroxidase (GPx), and the levels

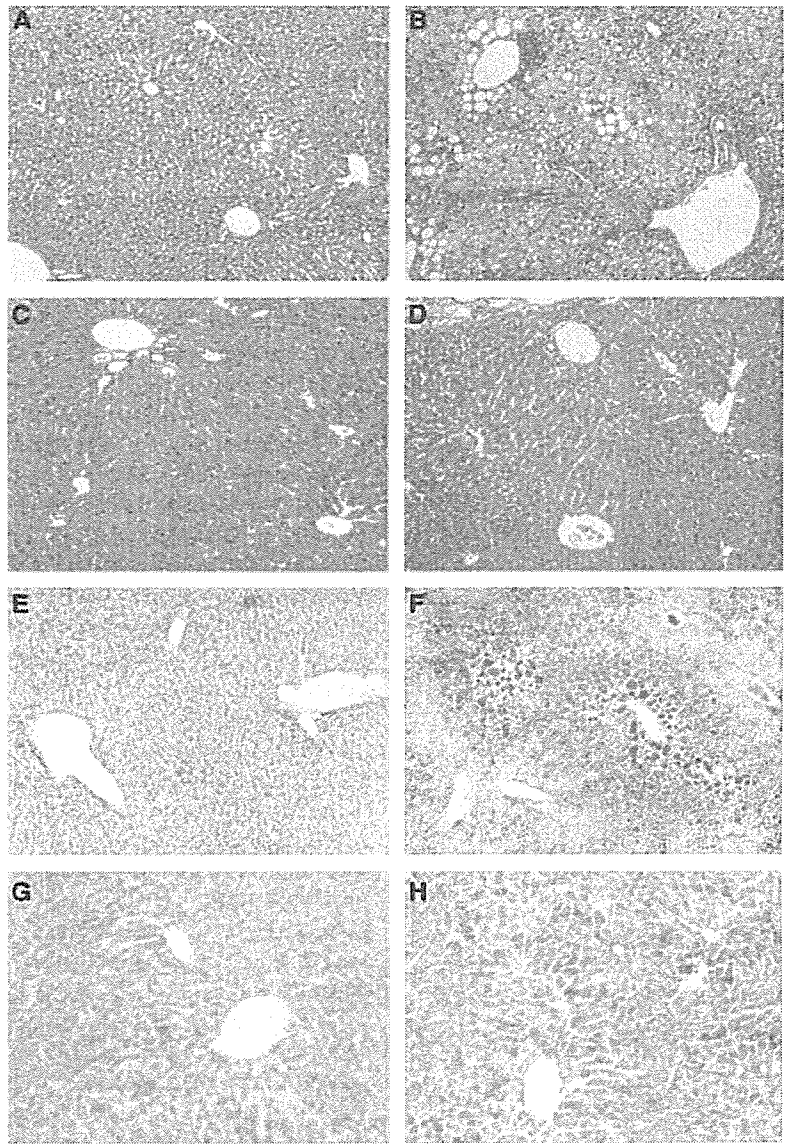

Fig. 1. Effects of fenofibrate on liver histology in DS (control) and FLS mice. Representative hematoxylin and eosin-stained (A–D) and oil red O-stained (E–H) liver sections (original magnification, × 100) from 15-week-old DS mice (A, C, E, G) and FLS mice (B, D, F, H) fed a normal diet (A, B, E, F) or a normal diet with 0.1% (w/w) fenofibrate (C, D, G, H) for 12 days.

Table 1. Effect of fenofibrate treatment on mouse body weight (BW), liver weight (LW), and biochemical Parameters in DS and FLS mice

	DS				FLS			
		15 W: fenofibrate				15 W: fenofibrate		
	13 W	(−)	(+)	*P*	13 W	(−)	(+)	*P*
BW (g)	39.3 ± 4.0	40.7 ± 5.4	36.2 ± 1.2	<0.05	36.5 ± 2.2	38.5 ± 1.1	36.6 ± 1.9	<0.05
LW (g)	1.9 ± 0.1	1.9 ± 0.2	3.7 ± 0.3	<0.001	2.1 ± 0.2	2.4 ± 0.3	3.1 ± 0.2	<0.001
LW/BW (%)	4.6 ± 0.4	4.6 ± 0.3	10.1 ± 0.6	<0.001	5.6 ± 0.4	6.2 ± 0.7	8.6 ± 0.4	<0.001
ALT (IU/l)	20 ± 4	17 ± 6	34 ± 15	<0.01	27 ± 5	45 ± 20	52 ± 22	NS
AST (IU/l)	74 ± 4	82 ± 6	74 ± 13	NS	62 ± 19	78 ± 18	69 ± 17	NS
TG (mg/dl)	200 ± 54	274 ± 85	23 ± 8	<0.001	289 ± 65	267 ± 61	74 ± 25	<0.001
FFA (μEQ/l)	252 ± 103	517 ± 134	134 ± 55	<0.001	250 ± 164	451 ± 80	158 ± 36	<0.001
T-chol (mg/dl)	106 ± 18	125 ± 18	71 ± 11	<0.001	141 ± 10	138 ± 16	145 ± 17	NS

NS, not significant; ALT, alanine aminotransferase; AST, aspartate aminotransferase; W, weeks; DS, dd Shionogi; FLS, fatty liver Shionogi.

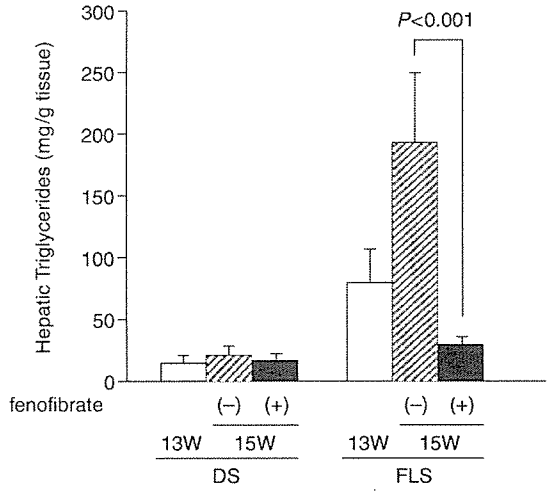

Fig. 2. Levels of hepatic triglyceride in 13-week-old DS and FLS mice and 15-week-old DS and FLS mice treated with or without fenofibrate for 12 days. Values represent the mean ± SD for eight mice in each group.

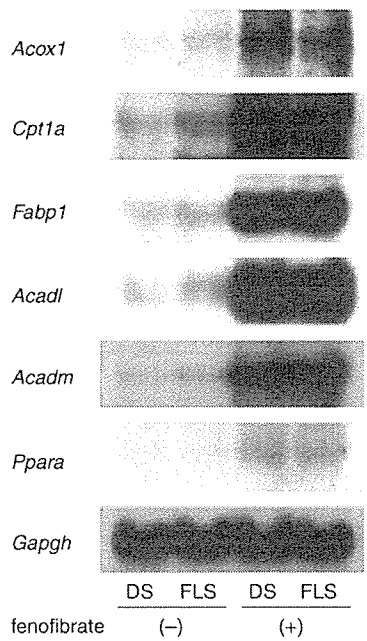

Fig. 3. Effects of fenofibrate on hepatic mRNA levels of genes involved in lipid turnover. Representative Northern blot analyses of *Acox1*, *Cpt1a*, *Fabp1*, *Acadl*, *Acadm*, and *Ppara*, using total RNA from livers of DS and FLS mice treated with or without fenofibrate. *Gapdh* served as a control probe.

of GSH, an endogenous antioxidant. Catalase activity was significantly lower in FLS mice than in DS mice; however, fenofibrate treatment in FLS mice induced catalase activity to the same level as seen in DS mice (Fig. 4B). On the other hand, no differences were observed in the levels of Cu/Zn-SOD, GPx, or GSH between the two strains of mice, and fenofibrate had no significant effects on the levels of any of these endogenous antioxidants (Fig. 4B). Northern blot analyses showed that fenofibrate upregulated mRNA levels of catalase (*Cat*) and Cu/Zn-SOD (*Sod1*) genes in both strains of mice (Fig. 5), and it induced the enzymatic activity of catalase but not Cu/Zn-SOD (Fig. 4B). These findings suggested that fenofibrate reduced lipid peroxidation in part by activating *Cat* expression.

Discussion

In the present study we demonstrated that short-term (12 days) treatment with fenofibrate, a PPARα agonist, dramatically improved steatosis in FLS mice (Fig. 1). Fenofibrate reduced hepatic triglyceride levels by activating expression of genes involved in fatty acid turnover (Figs 2 and 3). AOX (encoded by *Acox1*) and CPT-1 (*Cpt1a*) are rate-limiting enzymes in fatty acid oxidation (38, 39); L-FABP (*Fabp1*) plays a role in the influx of long-chain fatty acids into hepatocytes (40), LCAD (*Acadl*) and MCAD (*Acadm*) catalyze the initial step of fatty acid β-oxidation in mitochondria (41). Fenofibrate upfregulated the PPARα gene (*Ppara*), indicating a 'feed-forward' mechanism for activating its target genes (Fig. 3). Similar antisteatotic actions of PPARα agonists were observed in other NAFLD models, such as high-fat diet-fed mice (42), choline-deficient diet-fed mice (28), and A-ZIP/F-1 mice (27). Compared with those models, however, FLS mice are unique in that they do not develop obesity or diabetes mellitus (12).

Our results showed that lipid peroxidation occurred in the liver of FLS mice (Fig. 4A). There is abundant evidence to suggest that increased liver triglycerides lead to increased oxidative stress in the hepatocytes of animals and humans (37, 43). Oxidative stress results from an imbalance between pro-oxidant and antioxidant chemical species. The predominant pro-oxidant chemicals in fatty liver are molecules collectively referred to as reactive oxygen species (ROS). Increased production of ROS in the presence of excess free fatty acids has been observed in animal models of NASH (44, 45). On the other hand, the antioxidant capacity of the liver (GSH content, SOD, and catalase activities) was decreased in patients with NASH (46) and in animal models, such as ob/ob mice, which had hepatic steatosis (47). In FLS mice, the hepatic catalase activity was reduced compared with DS mice (Fig. 4B), although there was no difference in catalase mRNA levels between the two strains (Fig. 5).

Fenofibrate decreased hepatic lipid peroxidation in FLS mice (Fig. 4A). It was probable that the improvement in steatosis led to the decrease in

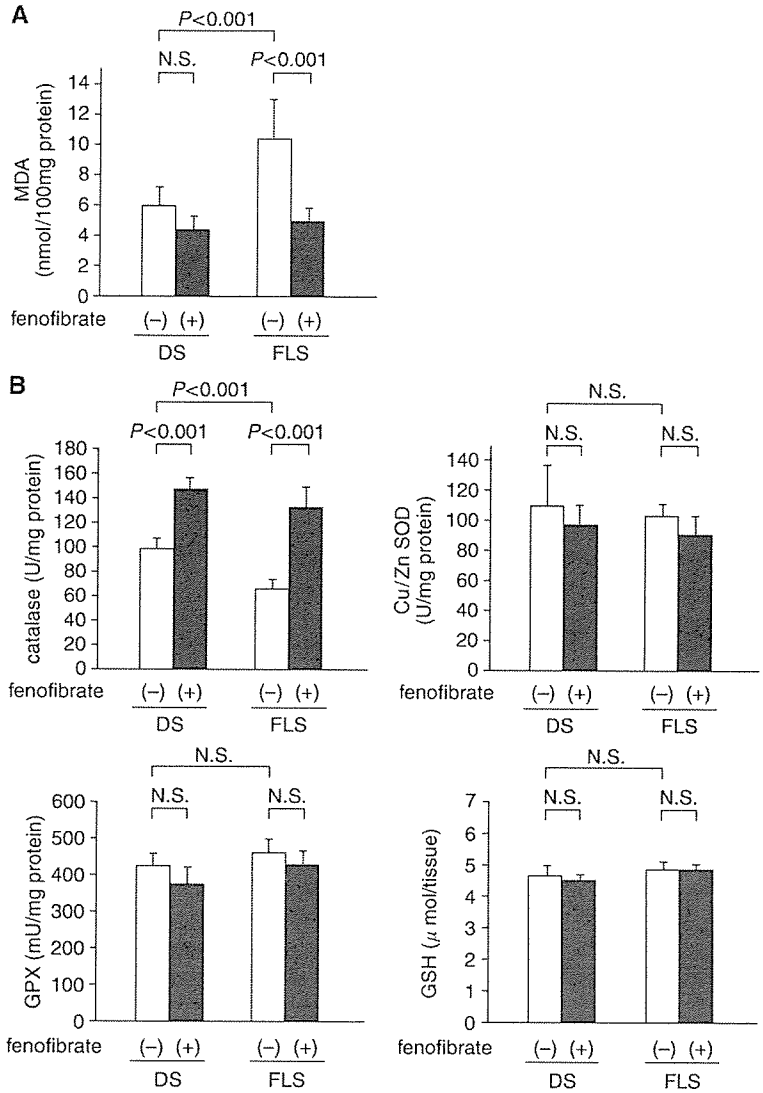

Fig. 4. (A) Levels of total hepatic malondialdehyde (MDA), a marker for lipid peroxidation, in livers of DS and FLS mice treated with or without fenofibrate. Values represent the mean ± SD for eight mice in each group. (B) Levels of antioxidant enzymes (catalase, Cu/Zn-SOD, and GPx) and GSH in the livers of DS and FLS mice treated with or without fenofibrate. Values represent the mean ± SD for eight mice in each group.

lipid peroxidation. Additionally, our findings suggested that the induction of catalase by fenofibrate also contributed to decreased lipid peroxidation (Fig. 4B). The peroxisome proliferator response element (PPRE), the binding site of PPAR, has been recently identified in the promoter region of the catalase gene (48). Indeed, our earlier study showed that Wy-14643, a PPARα agonist, upregulated expression of catalase mRNA in rats (29). Compatible with these observations, fenofibrate induced the transcription of the catalase gene in FLS mice in the present study (Fig. 5). Fenofibrate upregulated the expression of Cu/Zn-SOD mRNA without increasing its enzymatic activity (Figs 4 and 5). Other investigators also observed a discrepancy between mRNA levels and enzymatic activities of Cu/Zn-SOD (49, 50), although the reason for the discrepancy has not been determined.

Serum ALT levels were higher in FLS than DS mice, as expected. Although fenofibrate improved hepatic steatosis, it did not change ALT levels in FLS mice (Table 1). The agent slightly increased ALT levels in DS mice. It has been observed that fenofibrate administration increased ALT levels in several mouse and rat models by an as yet unresolved mechanism (51, 52). This effect of fenofibrate might counteract the results that it improved hepatic steatosis and decreased hepatic lipid peroxidation in FLS mice.

In conclusion, this study demonstrates that fenofibrate improves hepatic steatosis in FLS

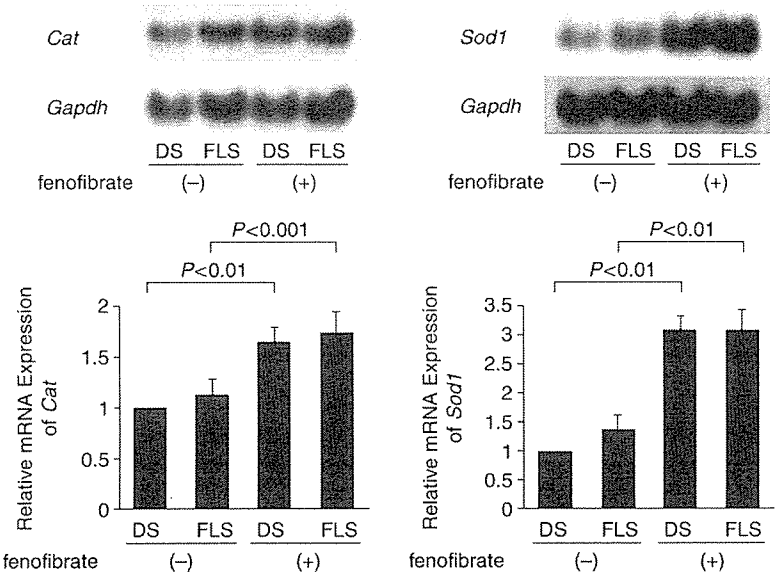

Fig. 5. Upper: representative Northern blots of the catalase (*Cat*) and Cu/Zn-SOD (*Sod1*) genes using total RNA from livers of DS and FLS mice treated with or without fenofibrate. *Gapdh* served as a control probe. Lower: relative expression levels of mRNA of the two genes were determined by image analysis. Values represent the mean ± SD of three independent experiments.

mice with hereditary fatty liver, probably through activation of genes involved in fatty acid turnover. Fenofibrate decreased lipid peroxidation in the liver of mice by improving steatosis and inducing catalase. Our results suggest that fenofibrate, which is currently used in the therapy of hyperlipidemia, might also be useful for treating patients with NAFLD, even in cases where NAFLD is not associated with obesity or diabetes mellitus.

References

1. Marchesini G, Bugianesi E, Forlani G, et al. Nonalcoholic fatty liver, steatohepatitis, and the metabolic syndrome. Hepatology 2003; 37: 917–23.
2. Marchesini G, Brizi M, Morselli-Labate A M, et al. Association of nonalcoholic fatty liver disease with insulin resistance. Am J Med 1999; 107: 450–5.
3. Chitturi S, Abeygunasekera S, Farrell G C, et al. NASH and insulin resistance: insulin hypersecretion and specific association with the insulin resistance syndrome. Hepatology 2002; 35: 373–9.
4. Wanless I R, Lentz J S. Fatty liver hepatitis (steatohepatitis) and obesity: an autopsy study with analysis of risk factors. Hepatology 1990; 12: 1106–10.
5. Bacon B R, Farahvash M J, Janney C G, Neuschwander-Tetri B A. Nonalcoholic steatohepatitis: an expanded clinical entity. Gastroenterology 1994; 107: 1103–9.
6. Yamauchi N, Itoh Y, Tanaka Y, et al. Clinical characteristics and prevalence of GB virus C, SEN virus, and HFE gene mutation in Japanese patients with nonalcoholic steatohepatitis. J Gastroenterol 2004; 39: 654–560.
7. Marchesini G, Brizi M, Bianchi G, et al. Nonalcoholic fatty liver disease: a feature of the metabolic syndrome. Diabetes 2001; 50: 1844–50.
8. Day C P, James O F. Steatohepatitis: a tale of two "hits"? Gastroenterology 1998; 114: 842–5.
9. Younossi Z M, Diehl A M, Ong J P. Nonalcoholic fatty liver disease: an agenda for clinical research. Hepatology 2002; 35: 746–52.
10. Reddy J K. Nonalcoholic steatosis and steatohepatitis. III. Peroxisomal beta-oxidation, PPAR alpha, and steatohepatitis. Am J Physiol Gastrointest Liver Physiol 2001; 281: G1333–9.
11. Chitturi S, Farrell G C. Etiopathogenesis of nonalcoholic steatohepatitis. Semin Liver Dis 2001; 21: 27–41.
12. Soga M, Kishimoto Y, Kawaguchi J, et al. The FLS mouse: a new inbred strain with spontaneous fatty liver. Lab Anim Sci 1999; 49: 269–75.
13. Soga M, Kishimoto Y, Kawamura Y, Inagaki S, Makino S, Saibara T. Spontaneous development of hepatocellular carcinomas in the FLS mice with hereditary fatty liver. Cancer Lett 2003; 196: 43–8.
14. Schoonjans K, Staels B, Auwerx J. The peroxisome proliferator activated receptors (PPARS) and their effects on lipid metabolism and adipocyte differentiation. Biochim Biophys Acta 1996; 1302: 93–109.
15. Desvergne B, Wahli W. Peroxisome proliferator-activated receptors: nuclear control of metabolism. Endocr Rev 1999; 20: 649–88.
16. Linden D, Alsterholm M, Wennbo H, Oscarsson J. PPARalpha deficiency increases secretion and serum levels of apolipoprotein B-containing lipoproteins. J Lipid Res 2001; 42: 1831–40.
17. Issemann I, Green S. Activation of a member of the steroid hormone receptor superfamily by peroxisome proliferators. Nature 1990; 347: 645–50.
18. Dreyer C, Krey G, Keller H, Givel F, Helftenbein G, Wahli W. Control of the peroxisomal beta-oxidation pathway by a novel family of nuclear hormone receptors. Cell 1992; 68: 879–87.
19. Kliewer S A, Forman B M, Blumberg B, et al. Differential expression and activation of a family of murine peroxisome proliferator-activated receptors. Proc Natl Acad Sci USA 1994; 91: 7355–9.

20. Braissant O, Foufelle F, Scotto C, Dauca M, Wahli W. Differential expression of peroxisome proliferator-activated receptors (PPARs): tissue distribution of PPAR-alpha, -beta, and -gamma in the adult rat. Endocrinology 1996; 137: 354–66.
21. Schoonjans K, Watanabe M, Suzuki H, et al. Induction of the acyl-coenzyme A synthetase gene by fibrates and fatty acids is mediated by a peroxisome proliferator response element in the C promoter. J Biol Chem 1995; 270: 19269–76.
22. Aoyama T, Peters J M, Iritani N, et al. Altered constitutive expression of fatty acid-metabolizing enzymes in mice lacking the peroxisome proliferator-activated receptor alpha (PPARalpha). J Biol Chem 1998; 273: 5678–84.
23. Kliewer S A, Xu H E, Lambert M H, Willson T M. Peroxisome proliferator-activated receptors: from genes to physiology. Recent Prog Horm Res 2001; 56: 239–63.
24. Forman B M, Chen J, Evans R M. Hypolipidemic drugs, polyunsaturated fatty acids, and eicosanoids are ligands for peroxisome proliferator-activated receptors alpha and delta. Proc Natl Acad Sci USA 1997; 94: 4312–7.
25. Hashimoto T, Fujita T, Usuda N, et al. Peroxisomal and mitochondrial fatty acid beta-oxidation in mice nullizygous for both peroxisome proliferator-activated receptor alpha and peroxisomal fatty acyl-CoA oxidase. Genotype correlation with fatty liver phenotype. J Biol Chem 1999; 274: 19228–36.
26. Grundy S M, Vega G L. Fibric acids: effects on lipids and lipoprotein metabolism. Am J Med 1987; 83: 9–20.
27. Chou C J, Haluzik M, Gregory C, et al. WY14,643, a peroxisome proliferator-activated receptor alpha (PPARalpha) agonist, improves hepatic and muscle steatosis and reverses insulin resistance in lipoatrophic A-ZIP/F-1 mice. J Biol Chem 2002; 277: 24484–9.
28. Ip E, Farrell G C, Robertson G, Hall P, Kirsch R, Leclercq I. Central role of PPARalpha-dependent hepatic lipid turnover in dietary steatohepatitis in mice. Hepatology 2003; 38: 123–32.
29. Toyama T, Nakamura H, Harano Y, et al. PPARalpha ligands activate antioxidant enzymes and suppress hepatic fibrosis in rats. Biochem Biophys Res Commun 2004; 324: 697–704.
30. Bligh E G, Dyer W J. A rapid method of total lipid extraction and purification. Can J Biochem Physiol 1959; 37: 911–7.
31. Beers R F Jr, Sizer I W. A spectrophotometric method for measuring the breakdown of hydrogen peroxide by catalase. J Biol Chem 1952; 195: 133–40.
32. Aebi H. Catalase in vitro. Methods Enzymol 1984; 105: 121–6.
33. Wan Y Y, Cai Y, Li J, et al. Regulation of peroxisome proliferator activated receptor alpha-mediated pathways in alcohol fed cytochrome P450 2E1 deficient mice. Hepatol Res 2001; 19: 117–30.
34. Grasso P. Hepatic changes associated with peroxisome proliferation. In: Gibson G, Lake B, eds. Peroxisomes: Biology and Importance in Toxicology and Medicine. London: Taylor and Francis, 1993; 639–52.
35. Cornwell P D, De Souza A T, Ulrich R G. Profiling of hepatic gene expression in rats treated with fibric acid analogs. Mutat Res 2004; 549: 131–45.
36. Minnich A, Tian N, Byan L, Bilder G. A potent PPAR alpha agonist stimulates mitochondrial fatty acid beta-oxidation in liver and skeletal muscle. Am J Physiol Endocrinol Metab 2001; 280: E270–9.
37. Letteron P, Fromenty B, Terris B, Degott C, Pessayre D. Acute and chronic hepatic steatosis lead to in vivo lipid peroxidation in mice. J Hepatol 1996; 24: 200–8.
38. Aoyama T, Tsushima K, Souri M, et al. Molecular cloning and functional expression of a human peroxisomal acyl-coenzyme A oxidase. Biochem Biophys Res Commun 1994; 198: 1113–8.
39. Britton C H, Mackey D W, Esser V, et al. Fine chromosome mapping of the genes for human liver and muscle carnitine palmitoyltransferase I (CPT1A and CPT1B). Genomics 1997; 40: 209–11.
40. Chan L, Wei C F, Li W H, et al. Human liver fatty acid binding protein cDNA and amino acid sequence. Functional and evolutionary implications. J Biol Chem 1985; 260: 2629–32.
41. Matsubara Y, Indo Y, Naito E, et al. Molecular cloning and nucleotide sequence of cDNAs encoding the precursors of rat long chain acyl-coenzyme A, short chain acyl-coenzyme A, and isovaleryl-coenzyme A dehydrogenases. Sequence homology of four enzymes of the acyl-CoA dehydrogenase family. J Biol Chem 1989; 264: 16321–3.
42. Mancini F P, Lanni A, Sabatino L, et al. Fenofibrate prevents and reduces body weight gain and adiposity in diet-induced obese rats. FEBS Lett 2001; 491: 154–8.
43. Browning J D, Horton J D. Molecular mediators of hepatic steatosis and liver injury. J Clin Invest 2004; 114: 147–52.
44. Hensley K, Kotake Y, Sang H, et al. Dietary choline restriction causes complex I dysfunction and increased H(2)O(2) generation in liver mitochondria. Carcinogenesis 2000; 21: 983–9.
45. Yang S, Zhu H, Li Y, et al. Mitochondrial adaptations to obesity-related oxidant stress. Arch Biochem Biophys 2000; 378: 259–68.
46. Videla L A, Rodrigo R, Orellana M, et al. Oxidative stress-related parameters in the liver of non-alcoholic fatty liver disease patients. Clin Sci (London) 2004; 106: 261–8.
47. Laurent A, Nicco C, Tran Van Nhieu J, et al. Pivotal role of superoxide anion and beneficial effect of antioxidant molecules in murine steatohepatitis. Hepatology 2004; 39: 1277–85.
48. Girnun G D, Domann F E, Moore S A, Robbins M E. Identification of a functional peroxisome proliferator-activated receptor response element in the rat catalase promoter. Mol Endocrinol 2002; 16: 2793–801.
49. Frendo J L, Therond P, Guibourdenche J, Bidart J M, Vidaud M, Evain-Brion D. Modulation of copper/zinc superoxide dismutase expression and activity with in vitro differentiation of human villous cytotrophoblasts. Placenta 2000; 21: 773–81.
50. Steinkuhler C, Sapora O, Carri M T, et al. Increase of Cu, Zn-superoxide dismutase activity during differentiation of human K562 cells involves activation by copper of a constantly expressed copper-deficient protein. J Biol Chem 1991; 266: 24580–7.
51. Sekiya M, Yahagi N, Matsuzaka T, et al. Polyunsaturated fatty acids ameliorate hepatic steatosis in obese mice by SREBP-1 suppression. Hepatology 2003; 38: 1529–39.
52. Price S C, Hinton R H, Mitchell F E, et al. Time and dose study on the response of rats to the hypolipidaemic drug fenofibrate. Toxicology 1986; 41: 169–91.

Available online at www.sciencedirect.com
ScienceDirect
Hepatology Research 36 (2006) 94–99
HEPATOLOGY RESEARCH
http://www.elsevier.com/locate/hepres

First phase viral kinetic parameters and prediction of response to interferon alpha-2b/ribavirin combination therapy in patients with chronic hepatitis C

Akiko Makiyama*, Yoshito Itoh, Kohichiroh Yasui, Kohjiroh Mori, Mika Okita, Mika Nakayama, Junko Yamaoka, Masahito Minami, Tomoki Nakajima, Takeshi Okanoue

Molecular Gastroenterology and Hepatology, Kyoto Prefectural University of Medicine, Graduate School of Medical Science, Kawaramachi-Hirokouji, Kamigyou-ku, Kyoto 602-8566, Japan

Received 17 January 2006; received in revised form 15 June 2006; accepted 3 July 2006
Available online 6 September 2006

Abstract

The aim of the present study was to assess parameters in early phase HCV dynamics for predicting the outcome of interferon (IFN)/ribavirin combination therapy in patients with chronic hepatitis C (CH-C). Sixty-five CH-C patients who received IFN alpha-2b/ribavirin combination therapy were enrolled. The serum levels of HCV RNA 0 h and 3 months after commencing therapy were serially quantified. HCV kinetic parameters such as quantity, ratio of decline, and half-life were analyzed. In genotype 1 patients, both the quantity and the ratio of decline of HCV RNA 24 h after the start of therapy were useful predictors of a poor response. No patients who had serum HCV RNA above 200 KIU/ml 24 h after the start of therapy achieved a sustained viral response (SVR). In genotype 2 patients, conversely, these two parameters were predictors of a sustained viral response. The efficacy of these parameters in predicting the outcome of therapy was comparable to that of the disappearance of HCV RNA from sera at 4 weeks. These results demonstrate that parameters of HCV kinetics 24 h after the start of therapy are useful for the early prediction of outcome in response to IFN alpha-2b/ribavirin combination therapy.

Keywords: Chronic hepatitis C; HCV kinetics; Interferon; Ribavirin; Early prediction

1. Introduction

Interferon (IFN) is used to treat patients with chronic hepatitis C (CH-C) worldwide. However, most patients with genotype 1b and high hepatitis C virus (HCV) loads did not benefit from IFN monotherapy. In recent years, IFN/ribavirin (Rib) and peginterferon/Rib combination therapy are often used to treat patients with genotype 1, however, more than half of the patients did not succeed in clearing HCV RNA from the sera [1,2].

IFN therapy is expensive, requires a long period of treatment, and sometimes is accompanied by severe adverse effects. Until recently, the most widely accepted factors for predicting the outcome of IFN or IFN/Rib combination therapy include HCV genotype, quantity of HCV RNA, mutations in the non-structural 5A (NS5A) region of HCV, histological staging, age, and duration of HCV infection before therapy [1–8]. The early identification of non-responders (NRs) soon after initiating the combination therapy is worthwhile because it provides an indication as to when it may be advisable to discontinue unnecessary therapy. Early identification of responders motivates patients to adhere to therapy.

In CH-C patients, a biphasic decline in the serum levels of HCV RNA after initiating IFN or IFN/Rib combination therapy is well known [9]. A third phase decline has also been recently reported [10]. The first phase decline occurs within 24 h of starting therapy, and it is thought to occur due

* Corresponding author. Tel.: +81 75 251 5519; fax: +81 75 251 0710.
E-mail address: akiko@koto.kpu-m.ac.jp (A. Makiyama).

1386-6346/$ – see front matter © 2006 Elsevier Ireland Ltd. All rights reserved.
doi:10.1016/j.hepres.2006.07.001

to the IFN-mediated direct reduction of HCV RNA from the sera. The second phase decline is observed after 24 h and is thought to reflect the death of HCV-infected hepatocytes. After starting IFN or IFN/Rib combination therapy, the disappearance of HCV RNA at 2, 4, or 12 weeks is a useful predictor of responsiveness to treatment [11–23] and the second phase HCV decline is associated with sustained response [24].

Several recent reports have indicated that the first phase viral decline is also useful for early prediction of the response to IFN or IFN/Rib combination therapy [25,26], however, a general consensus has not been obtained. In the present study, we investigated HCV kinetics in Japanese patients treated with IFN/Rib combination therapy and we confirmed that first phase viral kinetics are useful for predicting treatment outcome.

2. Methods

2.1. Patients

Sixty-five patients with CH-C were enrolled in this study. All patients were admitted to and followed at the outpatient clinic of the University Hospital of Kyoto Prefectural University of Medicine between December 2001 and September 2003. They consisted of 38 men and 27 women, ranging from 27 to 70 years old [54.2 ± 9.7 (mean ± S.D.)]. All patients were positive for anti-HCV antibody and serum HCV RNA and all had elevated serum alanine aminotransferase (ALT) levels for at least 6 months. They were also negative for hepatitis B virus surface antigen and human immunodeficiency virus. Patients who had co-existing liver diseases such as autoimmune hepatitis, primary biliary cirrhosis, or evidence for alcohol abuse were excluded from this study. Liver needle biopsy was performed prior to IFN therapy and the histological diagnoses were reached according to the classification of Desmet [27]. Sustained viral responders (SVRs) were defined as those who showed negative serum HCV RNA for 6 months after finishing the combination therapy. The rest of the patients were regarded as non-responders. Informed consent was obtained from all participants and the study protocol was approved by the ethical committee of the university.

2.2. Study protocol

Six MU of IFN alpha-2b (Intoron-A, Schering-Plough Corp., Kenilworth, NJ) was injected intramuscularly daily for 2 weeks, then switched to thrice weekly for 22 weeks in combination with Rib (Rebetol, Schering-Plough Corp., Kenilworth, NJ). Rib was given orally at a dose of either 800 mg (body weight ≥60 kg) or 600 mg (body weight <60 kg) daily for 24 weeks. Blood samples were obtained at 0, 6, 12 and 24 h; at 2, 4, 7, and 14 days; and at 1, 3, 6, and 12 months after the initiation of combination therapy.

2.3. Quantification and determination of HCV RNA and genotyping

Serum HCV RNA levels were determined by use of the Amplicor GT HCV monitor (Roche Diagnostic Systems, Tokyo, Japan). The detection range of this assay was between 0.5–850 KIU/ml. When the serum HCV RNA level was below 0.5 KIU/ml, the existence of serum HCV RNA was determined by reverse transcription-nested polymerase chain reaction (RT-nested PCR) using the Amplicor HCV v2.0 (Roche Diagnostic Systems, Tokyo, Japan), which had a detection limit of 50 IU/ml. HCV genotypes 1 and 2 were determined by a serologic genotyping assay [28–30]. Genotypes 1 and 2 in this assay correspond to genotypes 1 (1a, 1b) and 2 (2a, 2b) respectively proposed by Simmonds et al. [31].

2.4. HCV kinetic parameters

We determined the half-lives of HCV RNA in the first and second phases using logarithmic approximate curves for the two phases. Samples containing HCV RNA greater than 850 KIU/ml or less than 0.5 KIU/ml were omitted from the curve and the upward curves were also omitted.

2.5. Statistical analysis

Positive predictive value (PPV) was calculated as the percentage of SVRs among patients who were predicted to have a sustained viral response (SVR). Negative predictive value (NPV) was calculated as the percentage of NRs among patients not meeting the criteria for prediction of a SVR. p-values were calculated by Fischer's exact probability test and Mann–Whitney U-test. Statistical significance was set at $p < 0.05$.

3. Results

Baseline characteristics of 65 chronic hepatitis C patients (49 genotype 1 patients and 16 genotype 2 patients) who received IFN/Rib combination therapy were shown in Table 1. As have been already known [3–6], SVRs had less advanced staging, lower HCV load, and increased ratio of genotype 2.

HCV dynamics during combination therapy are presented in four groups depending on the genotype and response to the therapy (Fig. 1A–D). In genotype 1 patients, the mean half-life of HCV RNA in the first phase was 5.5 ± 1.5 h in SVRs, which was significantly ($p = 0.0361$) shorter than that of NRs (9.8 ± 10.0 h). The mean half-life of HCV RNA in the second phase was 121.4 ± 104.2 h in SVRs, which was also significantly ($p = 0.0003$) shorter than that of NRs (470.0 ± 752.3 h). Although the half-life of HCV RNA in SVRs in both the first and second phase was significantly shorter than that of genotype 1 patients who were NRs, the

Table 1
Characteristic of chronic hepatitis C patients

	SVR ($n=23$)	NR ($n=42$)	p
Gender (male/female)	13/10	25/17	>0.9999
Age (years)[a]	55.2 ± 6.9	53.6 ± 11.0	0.9890
Weight (kg)[a]	61.4 ± 10.3	64.3 ± 10.3	0.2301
BMI[a]	23.0 ± 2.6	23.9 ± 2.6	0.1514
ALT (IU/ml)[a]	122.4 ± 79.9	122.4 ± 103.8	0.6706
AST (IU/ml)[a]	88.1 ± 42.9	98.2 ± 79.6	0.8584
PLT ($\times 10^4/\mu l$)[a]	16.3 ± 5.6	14.0 ± 5.0	0.1765
Fibrosis (stage)			
1	7	7	
2	10	15	0.0398
3	4	18	
Not available	2	2	
Viral load (KIU/ml)[a]	440.3 ± 308.3	669.6 ± 197.7	0.0066
Genotype (1/2)	10/13	39/3	<0.0001

ALT: alanine aminotransferase; AST: aspartate aminotransferase; BMI: body mass index; SVR: sustained viral responder (serum HCV RNA was negative after 6 months from the end of therapy); NR: non-responder (serum HCV RNA was positive after 6 months from the end of therapy).

[a] Data are expressed as mean ± S.D. p-values were calculated by Fischer's exact probability test and Mann–Whitney U-test.

Table 2
Mean half-life of HCV dynamics during combination therapy

	SVR	NR	p
Genotype 1, $n=49$	$n=10$	$n=39$	
First phase (hour)	5.5 ± 1.5	9.8 ± 10.0	0.0361
Second phase (hour)	121.4 ± 104.2	470.0 ± 752.3	0.0003
Genotype 2, $n=16$	$n=13$	$n=3$	
First phase (hour)	5.8 ± 4.2	9.1 ± 1.4	0.0693
Second phase (hour)	110.9 ± 124.9	437.9 ± 320.6	0.0734

First phase is from before IFN therapy to 24 h after the start of combination therapy. Second phase is from 24 h to 3 months after the initiation of therapy. p-values were calculated by Mann–Whitney U-test.

half-life of HCV RNA in genotype 2 patients did not differ significantly between SVRs and NRs partly because of the small number of patients with genotype 2 (Table 2).

Among the 49 patients with genotype 1, 8 patients were negative for serum HCV RNA after 4 weeks of treatment, and a SVR was achieved in 5 of 8 patients. The PPV, as determined from the disappearance of serum HCV RNA after 4 weeks of treatment was 62.5% for SVRs, and the NPV was 90.2%. Six patients showed serum HCV RNA levels less than 5.0 KIU/ml after the first 24 h of therapy, and SVR was achieved in 4 patients. The PPV determined using HCV RNA levels less

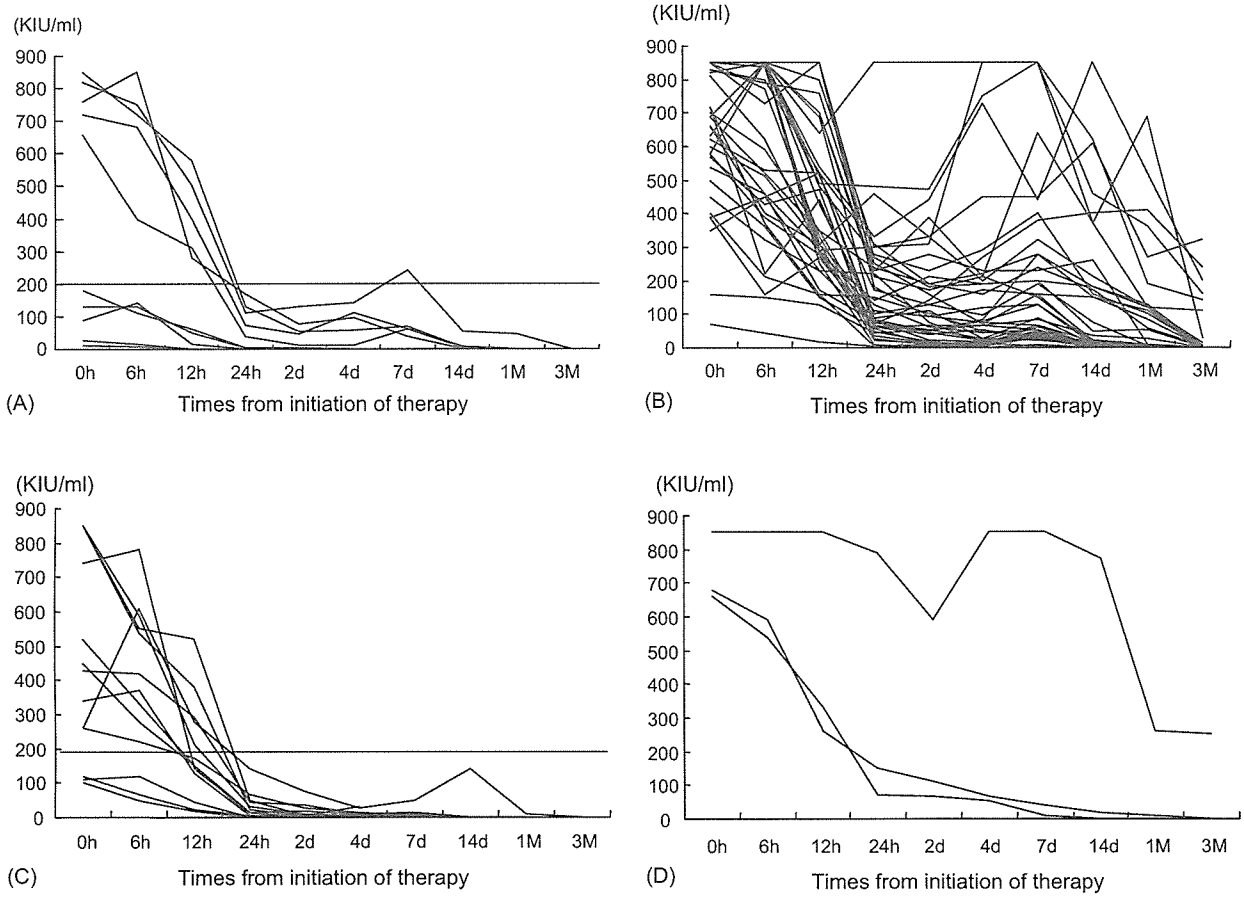

Fig. 1. (A–D) Serum HCV RNA dynamics during the first 3 months of IFN alpha-2b and Rib combination therapy. (A) Sustained viral responders (SVRs) in genotype 1. (B) Non-responders (NR) in genotype 1. (C) Sustained viral responders (SVR) in genotype 2. (D) Non- responders (NR) in genotype 2.

Table 3
Predicting SVR and NR using HCV kinetics

Criteria for SVR prediction	PPV (%)	NPV (%)	Sensitivity (%)	Specificity (%)
Genotype 1 ($n=49$)				
Negative for serum HCV RNA after 4 week of treatment	62.5 (5/8)	90.2 (37/41)	50.0 (5/10)	94.9 (36/39)
Viral levels at 24 h after the initiation of therapy <5.0 KIU/ml	66.7 (4/6)	86.0 (37/43)	40.0 (4/10)	94.9 (37/39)
The ratio of decrease in serum HCV RNA (24 h/0 h) >1.5 log	36.8 (7/19)	90.0 (27/30)	70.0 (7/10)	69.2 (27/39)
Genotype 2 ($n=16$)				
Negative for serum HCV RNA after 4 week of treatment	100 (10/10)	50.0 (3/6)	76.9 (10/13)	100 (3/3)
Viral levels at 24 h after the initiation therapy <50 KIU/ml	100 (12/12)	75.0 (3/4)	92.3 (12/13)	100 (3/3)
The ratio of decrease in serum HCV RNA (24 h/0 h) >1 log	100 (10/10)	50.0 (3/6)	76.9 (10/13)	100 (3/3)

PPV: positive predictive value (% meeting the criteria for SVR prediction that were SVR). NPV: negative predictive value (% not meeting the criteria for SVR prediction that were NR).

than 5.0 KIU/ml after the first 24 h of the therapy was 66.7%, and the NPV was 86.0%. Decrease in the serum levels of HCV RNA (24 h/0 h) greater than 1.5 log were seen in 19 patients, and SVR was achieved in 7 patients. The PPV calculated based on the decrease in serum HCV RNA (24 h/0 h) was 36.8% in SVRs, and NPV was 90.0% (Table 3).

In genotype 2 patients, HCV dynamics did not differ significantly between SVRs and NRs at either phase. Among the 16 patients with genotype 2, 10 patients who had negative serum HCV RNA after 4 weeks of treatment all achieved SVR. The PPV calculated using negative serum HCV RNA after 4 weeks of treatment was 100% in SVRs, and the NPV was 50.0%. Twelve patients with serum HCV RNA levels lower than 50 KIU/ml after the first 24 h of treatment all achieved SVR. The PPV of SVRs, as determined using serum HCV RNA levels lower than 50 KIU/ml after the first 24 h of treatment, was 100%, and the NPV was 75.0%. Decrease in serum HCV RNA levels (24 h/0 h) greater than 1.0 log was seen in 10 patients and all of them achieved SVR. The PPV of SVRs, determined by a decrease in serum HCV RNA (24 h/0 h) of greater than 1.0 log was 100%, and the NPV was 50.0% (Table 3).

Because patients with genotype 1 and high HCV load showed a poor response to IFN/Rib combination therapy, we assessed the HCV load threshold in genotype 1 SVRs before or early after starting the combination therapy. Before therapy, the maximum serum HCV RNA level in SVRs was greater than 850 KIU/ml, which demonstrated that IFN/Rib combination therapy was effective in some patients with genotype 1 and very high HCV load. After initiating the combination therapy, the maximum serum HCV RNA levels in genotype 1 SVRs were 170 KIU/ml (24 h), 130 KIU/ml (2 d) and 140 KIU/ml (4 d) (Fig. 1A). Among genotype 1 patients, those who showed serum HCV RNA levels greater than 200 KIU/ml at 24 h after starting combination therapy did not achieve SVR (Fig. 1A).

4. Discussion

Biphasic decline in the serum levels of HCV RNA during IFN therapy for CH-C was reported by our group [9] and Neumann et al. [32]. Subsequent studies showed the second phase decline in the serum HCV RNA level to be an excellent predictor of SVR in IFN mono-therapy [24] and IFN/Rib combination therapy. For CH-C patients as well as for their physicians, easy evaluation of the probability of SVR/non-response (NR) soon after starting therapy is desirable both from a financial and emotional standpoint.

In the present study, we showed that HCV viral load and viral decline within the first 24 h are good predictors of NR in genotype 1 patients. These parameters are also good predictors of SVR in genotype 2 patients receiving IFN/Rib combination therapy, and their predictive value was comparable to that of the disappearance of HCV RNA from the sera after the first 4 weeks of treatment (Table 3).

Our findings are consistent with previous reports by Jessner et al. [25,33] who demonstrated that NR to IFN/Rib combination therapy could be predicted when the HCV viral load declined by less than 70% of baseline levels after a singe injection of 5 MU of IFN alpha-2b [25] and that the decline in viral load 24 h after a single test dose of standard IFN had also high predictive value for the outcome of peginterferon alpha-2a/Rib combination therapy [33]. Layden et al. [26] reported that only those patients with 24 h viral load less than 250 KIU/ml and 24 h viral declines of greater than 98% after 7.5–15 μg/ml consensus IFN achieve SVR [26]. The authors therefore advocated the use of the 250 KIU/ml at 24 h of the therapy threshold for achieving SVR. Karino et al. [34] reported that the decline in serum HCV RNA levels 24 h after the first injection of IFN was regulated by HCV genotypes and the extent of hepatic fibrosis [34]. In the present study, however, hepatic fibrosis had no relation to the 24 h viral load or viral decline (data not shown).

One of the most important effects of Rib on HCV dynamics is that it shortens the half-life of serum HCV RNA in the second phase of IFN/Rib combination therapy. It is therefore unlikely that Rib would have exerted a significant influence on the decline of serum HCV RNA after a single oral administration. There are at least two explanations for why HCV RNA levels after the first injection of IFN can predict the effectiveness of combination therapy. Firstly, serum HCV RNA levels may have to be below a certain threshold at the first phase of HCV kinetics during IFN/Rib combination therapy

to eradicate HCV in the second phase. Secondly, individual sensitivity to IFN may regulate the antiviral effect of IFN/Rib combination therapy.

Forns et al. [35] reported that "a viral load decrease of ≥2 log 10 at week 4 was the strongest predictor of virological response, when HCV-infected cirrhotic patients awaiting liver transplantation were treated with IFN/Rib combination therapy" [35]. Early prediction of the outcome at 24 h after starting IFN/Rib combination therapy may also be useful for avoiding unnecessary therapy prior to liver transplantation when IFN and Rib is administered to HCV-positive patients with liver cirrhosis or HCC whose white blood cells or platelet counts are reduced. It also motivates those patients who are likely to clear HCV before transplantation to adhere to the therapy. Further studies are required to clarify these issues.

We assessed the utility of evaluating the probability of SVR/NR soon after starting therapy and we found that those patients with serum HCV RNA levels greater than 200 KIU/ml at 24 h after starting combination therapy did not achieve SVR (Fig. 1A and C). This threshold of HCV RNA is recommended because patients with a low probability of SVR could be judged easily. Unexpectedly, patients with greater than 850 KIU/ml of HCV genotype 1b were verified to be capable of achieving SVR when the serum HCV RNA levels were lower than 200 KIU/ml at 24 h after the initiation of therapy.

In conclusion, quantity and the ratio of decline of HCV RNA after the first 24 h of the IFN/Rib combination therapy were a useful predictor of NR in genotype 1 patients and an accurate predictor of SVR in genotype 2 patients. No patients with serum HCV RNA greater than 200 KIU/ml 24 h after starting therapy achieved SVR. These results demonstrate the usefulness of HCV kinetic parameters after 24 h of therapy for the early prediction of the outcome of IFN alpha-2b/Rib combination therapy. In Japan, standard therapy for chronic hepatitis C patients with genotype 1 and high viral load had been the IFN/ribavirin combination therapy with around 20% of SVR rate until December 2004. With the advent of peginterferon/ribavirin combination therapy for 48 weeks, which is the standard therapy for these patients now in Japan, SVR rate has risen to approximately 50%. Now, the early prediction of the response to peginterferon/Rib combination therapy in patients with CH-C is under investigation.

References

[1] Manns MP, McHutchison JG, Gordon SC, et al. Peginterferon alfa-2b plus ribavirin compared with interferon alfa-2b plus ribavirin for initial treatment of chronic hepatitis C: a randomized trial. Lancet 2001;358:958–65.

[2] Fried MW, Shiffman ML, Reddy KR, et al. Peginterferon alfa-2a plus ribavirin for chronic hepatitis C virus infection. N Engl J Med 2002;347:975–82.

[3] Martinot-Peignoux M, Marcellin P, Pouteau M, et al. Pretreatment serum hepatitis C virus RNA levels and hepatitis C virus genotype are the main and independent prognostic factors of sustained response to interferon alfa therapy in chronic hepatitis C. Hepatology 1995;22:1050–6.

[4] Tsubota A, Chayama K, Ikeda K, et al. Factors predictive of response to interferon-alpha therapy in hepatitis C virus infection. Hepatology 1994;19:1088–94.

[5] Yamada G, Takatani M, Kishi F, et al. Efficacy of interferon alfa therapy in chronic hepatitis C patients depends primarily on hepatitis C virus RNA level. Hepatology 1995;22:1351–4.

[6] Shiratori Y, Kato N, Yokosuka O, et al. Predictors of the efficacy of interferon therapy in chronic hepatitis C virus infection. Tokyo-Chiba Hepatitis Research Group. Gastroenterology 1997;113:558–66.

[7] Enomoto N, Sakuma I, Asahina Y, et al. Mutations in nonstructural protein 5A gene and response to interferon in patients with chronic hepatitis C virus 1b infection. N Engl J Med 1996;334:77–81.

[8] Murakami T, Enomoto N, Kurosaki M, et al. Mutations in nonstructural protein 5A gene and response to interferon in hepatitis C virus genotype 2 infection. Hepatology 1999;30:1045–53.

[9] Yasui K, Okanoue T, Murakami Y, et al. Dynamics of hepatitis C viremia following interferon-α administration. J Infect Dis 1998;177:1475–9.

[10] Herrmann E, Lee JH, Marinos G, Modi M, et al. Effect of ribavirin on hepatitis C viral kinetics in patients treated with pegylated interferon. Hepatology 2003;37:1351–8.

[11] Castro FJ, Esteban JI, Juarez A, et al. Early detection of nonresponse to interferon puls ribavirin combination treatment of chronic hepatitis C. J Viral Hepatol 2002;9:202–7.

[12] Brouwer JT, Hansen BE, Niesters HG, Schalm SW. Early prediction of response in interferon monotherapy and in interferon-ribavirin combination therapy for chronic hepatitis C: HCV RNA at 4 weeks versus ALT. J Hepatol 1999;30:192–8.

[13] Di Marco V, Ferraro D, Almasio P, et al. Early viral clearance and sustained response in chronic hepatitis C: a controlled trial of interferon and ribavirin after high-dose interferon induction. J Viral Hepat 2002;9:354–9.

[14] McHutchison JG, Shad JA, Gordon SC, et al. Predicting response to initial therapy with interferon plus ribavirin in chronic hepatitis C using serum HCV RNA results during therapy. J Viral Hepat 2001;8: 414–20.

[15] Castro FJ, Esteban JI, Sauleda S, et al. Utility of early testing for HCV viremia as predictive factor of sustained response during interferon or interferon plus ribavirin treatment. J Hepatol 2000;32:843–9.

[16] Rosen HR, Ribeiro RR, Weiberger L, et al. Early hepatitis C viral kinetics correlate with long-term outcome in patients receiving high dose induction followed by combination interferon and ribavirin therapy. J Hepatol 2002;37:124–30.

[17] McHutchison J, Blatt L, Sedghi-Vaziri A, Russell J, Schmid P, Conrad A. Is there an optimal time to measure quantitative HCV RNA to predict non-response following interferon treatment for chronic HCV infection? J Hepatol 1998;29:362–8.

[18] Kakumu S, Aiyama T, Okumura A, Iwata K, Ishikawa T, Yoshioka K. Earlier loss of hepatitis C virus RNA in interferon therapy can predict a long-term response in chronic hepatitis C. J Gastroenterol Hepatol 1997;12:468–72.

[19] Orito E, Mizokami M, Suzuki K, et al. Loss of serum HCV RNA at week 4 of interferon-alfa therapy is associated with more favorable long-term response in patients with chronic hepatitis C. J Med Virol 1995;46:109–15.

[20] Knolle PA, Kremp S, Hohler T, Krummenauer F, Schirmacher P, Gerken G. Viral and host factors in the prediction of response to interferon-alpha therapy in chronic hepatitis C after long-term follow-up. J Viral Hepat 1998;5:399–406.

[21] Karino Y, Toyota J, Sugawara M, et al. Early loss of serum hepatitis C virus RNA can predict a sustained response to interferon therapy in patients with chronic hepatitis C. Am J Gastroenterol 1997;92:61–115.

[22] Zeuzem S, Lee JH, Franke A, et al. Quantification of the initial decline of serum hepatitis C virus RNA and response to interferon alfa. Hepatology 1998;27:1149–56.

[23] Gavier B, Martinez-Gonzalez MA, Reizu-Boj JI, et al. Viremia after one month of interferon therapy predicts treatment outcome in patients with chronic hepatitis C. Gastroenterology 1997;113:1647–53.
[24] Layden TJ, Mika B, Wiley TE. Hepatitis C kinetics: mathematical modeling of viral response to therapy. Semin Liver Dis 2000;20:173–83.
[25] Jessner W, Gschwantler M, Steindl-Munda P, et al. Primary interferon resistance and treatment response in chronic hepatitis C infection: a pilot study. Lancet 2001;358:1241–2.
[26] Layden JE, Layden TJ, Reddy KR, Levy-Drummer RS, Poulakos J, Neumann AU. First phase viral kinetic parameters as predictors of treatment response and their influence on the second phase viral decline. J Viral Hepat 2002;9:340–5.
[27] Desmet VJ. Histological classification of chronic hepatitis. Acta Gastroenterol Belg 1997;60:259–67.
[28] Tsukiyama-Kohara K, Yamaguchi K, Maki N, et al. Antigenicities of Group 1 and 2 hepatitis C virus polypeptides: molecular basis of diagnosis. Virology 1993;192:430–7.
[29] Tanaka T, Tsukiyama-Kohara K, Yamaguchi K, et al. Significance of specific antibody assay for genotyping of hepatitis C virus. Hepatology 1994;19:1347–53.
[30] Kohara M, Tanaka T, Tsukiyama-Kohara K, et al. Hepatitis C virus genotypes 1 and 2 respond to interferon-alpha with different virologic kinetics. J Infect Dis 1995;172:934–8.
[31] Simmonds P, Alberti A, Alter HJ, et al. A proposed system for the nomenclature of hepatitis C viral genotypes. Hepatology 1994;19:1321–4.
[32] Neumann AU, Lam NP, Dahari H, et al. Hepatitis C viral dynamics in vivo and the antiviral efficacy of interferon-alpha therapy. Science 1998;2:103–7.
[33] Jessner W, Stauber R, Hackl F, et al. Early viral kinetics on treatment with pegylated interferon-alpha-2a in chronic hepatitis C virus genotype 1 infection. J Viral Hepat 2003;10:37–42.
[34] Karino Y, Toyota J, Sugawara M, et al. Hepatitis C virus genotypes and hepatic fibrosis regulate 24-h decline of serum hepatitis C virus RNA during interferon therapy in patients with chronic hepatitis C. J Gastroenterol Hepatol 2003;18:404–10.
[35] Forns X, Garcia-Retortillo M, Serrano T, et al. Antiviral therapy of patients with decompensated cirrhosis to prevent recurrence of hepatitis C after liver transplantation. J Hepatol 2003;39:389–96.

Journal of Medical Virology 78:341–352 (2006)

Clinical and Virological Features of Non-Breakthrough and Severe Exacerbation Due to Lamivudine-Resistant Hepatitis B Virus Mutants

Fumitaka Suzuki,[1,2]* Norio Akuta,[1] Yoshiyuki Suzuki,[1] Hitomi Sezaki,[1] Yasuji Arase,[1] Tetsuya Hosaka,[1] Takashi Someya,[1] Masahiro Kobayashi,[1] Satoshi Saitoh,[1] Kenji Ikeda,[1] Mariko Kobayashi,[3] Marie Matsuda,[3] Junko Satoh,[3] Sachiyo Watahiki,[3] and Hiromitsu Kumada[1]

[1]*Department of Gastroenterology, Toranomon Hospital, Tokyo, Japan*
[2]*Okinaka, Memorial Institute for Medical Research, Tokyo, Japan*
[3]*Research Institute for Hepatology, Toranomon Branch Hospital, Kawasaki, Japan*

Patients who develop YMDD mutant during lamivudine therapy for hepatitis B virus (HBV) infection exhibit various clinical courses. Some patients show normal ALT levels, whereas others develop severe hepatitis exacerbations (SHEs) due to YMDD mutants. We studied 136 patients with YMDD mutant among 362 Japanese adult patients on lamivudine therapy. Clinical and virological features of patients without elevated HBV DNA after emergence of YMDD mutant (non-elevated group) were investigated. Moreover, virological analysis was also performed in patients with SHE due to YMDD mutants. Patients in the non-elevated group were characterized by HBeAg-negative pretreatment, HBeAg loss during therapy, a longer duration from commencement of therapy until emergence of YMDD mutant, and no mixed-type YMDD mutants. Patients with SHE had more substitutions in the reverse transcriptase (rt) region within the polymerase gene at the time of exacerbation than those without SHE, although no specific substitutions were noted. Sequence analysis of full-length HBV genome showed more substitutions in X, rt, and surface proteins in patients with SHE than in those without elevated HBV DNA level. In conclusion, negativity for HBeAg at commencement of therapy or before emergence of YMDD mutant was an important factor among non-elevated group. More substitutions in the rt region and the other proteins may be related to the emergence of severe hepatitis caused by lamivudine-resistant virus. ***J. Med. Virol. 78:341–352, 2006.*** © 2006 Wiley-Liss, Inc.

KEY WORDS: HBV; breakthrough hepatitis; YMDD mutant; reverse transcriptase

INTRODUCTION

Hepatitis B virus (HBV) infection is a common disease that can lead to a chronic carrier state, and is associated with the risk of development of progressive disease and hepatocellular carcinoma [Beasley et al., 1981]. Several studies have reported the effectiveness of a number of nucleoside analogs, such as lamivudine in the suppression of HBV replication, improvement of transaminase levels and liver histology, and enhancement of the rate of loss of hepatitis B e antigen (HBeAg) [Dienstag et al., 1995, 1999; Lai et al., 1998; Suzuki et al., 1999]. A major problem with the long-term use of lamivudine, however, is the potential development of viral resistance, associated with increases in HBV DNA and serum transaminases. Long-term lamivudine therapy may therefore increase the likelihood of the development of resistance [Nafa et al., 2000; Suzuki et al., 2003].

HBV polymerase can be divided into several functional domains, which have been designated the 'fingers,' 'palm,' and 'thumb' sub-domains by comparison with the reverse transcriptase (rt) of human immunodeficiency virus [Das et al., 2001]. The YMDD motif is located in the palm sub-domain, which is thought to contain the major catalytic nucleus of the polymerase, while the fingers sub-domain contains the region that overlaps the 'a-determinant' of hepatitis surface antigen (HBsAg) [Torresi et al., 2002a]. The polymerase gene completely overlaps the surface gene, resulting in the potential to significantly alter the activity of the

Grant sponsor: Ministry of Health, Labor and Welfare, Japan.

*Correspondence to: Fumitaka Suzuki, MD, Toranomon Hospital, Department of Gastroenterology, 2-2-2 Toranomon, Minato-ku, Tokyo 105-8470, Japan. E-mail: fumitakas@toranomon.gr.jp

Accepted 7 November 2005
DOI 10.1002/jmv.20546
Published online in Wiley InterScience (www.interscience.wiley.com)